Available online at www.sciencedirect.com

SCIENCE DIRECT®

Ore Geology Reviews 29 (2006) 1–18

ORE GEOLOGY REVIEWS

www.elsevier.com/locate/oregeorev

Geophysical and petrophysical study of an iron oxide copper gold deposit in northern Sweden

Alessandro Sandrin *, Sten-Åke Elming

Division of Applied Geophysics, Department of Environmental Engineering, Luleå University of Technology, SE-97187, Luleå, Sweden

Received 19 December 2003; accepted 16 June 2005
Available online 12 September 2005

Abstract

A geophysical–petrophysical study has been performed in an area WSW of the city of Kiruna, northern Sweden. The sub-regional tectonic setting is dominated by two important shear zones, which define the boundary of a granitic body. Many Cu–Fe-occurrences are located in proximity of faults related to these major deformation zones. Particular attention has been given to the Tjårrojåkka iron oxide copper gold (IOCG) deposit. Here the bedrock is characterised by intermediate to mafic meta-volcanics, metamorphosed intermediate to mafic dykes, and gabbroic–dioritic intrusions of Svecofennian ages (~1.96–1.75 Ga). The major Cu- and Fe-occurrences are hosted by the meta-andesites. The aim of the study is to put the deposits into a tectonic framework and test existing hypotheses for their occurrences.

Glacial deposits cover almost the entire area, leading to a scarcity of outcrops and inferring that geophysical data are fundamental for geological understanding. In addition to this, petrophysical analysis is vital for the interpretation of geophysical data (gravity, airborne magnetics and radiometrics, very low frequency) and for the definition of geophysical signatures of the deposits. The anisotropy of magnetic susceptibility (AMS) was also studied for the tectonic analysis. More than 150 oriented samples were collected in a number of outcrops along a profile intersecting the major structures in the Tjårrojåkka area.

From the airborne magnetic data, two major linear features are interpreted as deformation zones. The strike of these deformation zones is approximately NW–SE and E–W, respectively. The same trends have been defined from other geophysical data such as airborne VLF and ground gravity data. A third important structural trend striking SW–NE has been defined by K/Th data and ground magnetic data. Very good agreement has been found between geophysical lineaments and AMS directions. Magnetic foliations determined by AMS measurements confirm the existence of three major trends in the study area: SW–NE, E–W and NW–SE. The major Fe-orebody shows approximately a SW–NE strike direction as defined from ground magnetic data. This is parallel to the strike of magnetic foliation determined in outcrops ~1 km NW of the deposit. The epigenetic nature of the Cu and Fe occurrences in Tjårrojåkka and their spatial relationship with deformation zones suggest a connection between the formation of the deposits and a tectonic event. A later tectonic episode resulted in E–W trending deformation in the central area, affecting the orebodies themselves. Other, probable, compressive deformations have been indicated from petrophysical and geophysical analyses.

* Corresponding author. Current address: Geological Institute, University of Copenhagen, Oster Voldgade 10, DK-1350, Copenhagen, Denmark. Fax: +45 33 14 83 22.

E-mail address: ALSA@geol.ku.dk (A. Sandrin).

doi:10.1016/j.oregeorev.2005.06.001

Thermomagnetic measurements indicate that Fe-oxides (Ti-magnetite) are common in the area, while Fe-sulphides are almost absent. Multi-domain magnetite has been identified as the most common Fe-oxide in different rock types, while an unstable magnetic mineral has been detected in metamorphosed volcanics. A good spatial correlation has been observed between Cu-deposits and high K/Th values from radiometric data, values that are expressions of potassic alteration.

Keywords: Precambrian; Fe–Cu–(Au) deposits; Tectonics; Petrophysics; Geophysics; Anisotropy of magnetic susceptibility (AMS); Tjårrojåkka, Sweden

1. Introduction

Iron oxide copper–gold (IOCG) deposits have attracted the interest of ore geologists since the discovery, in 1976, of the giant Olympic Dam deposit in South Australia. Hitzman et al. (1992) summarised the geological characteristics of this "new" class of deposits, and included within it, as a "subset", the previously known apatite–iron ores (Kiruna-type). Hitzman et al. (1992) also included the Tjårrojåkka occurrences, northern Sweden, into the group of Proterozoic Fe oxide (Cu–U–REE–Au) deposits in the Stuor–Ratek district, 50 km SW of Kiruna. The Tjårrojåkka area, investigated in the past, but still with many unsolved problems, has been selected for a detailed geological, geophysical and petrophysical study. The purpose of this study is principally to put the deposits into a tectonic framework combining usual geophysical methods with the analysis of petrophysical properties. Airborne magnetic, radiometric and VLF data, as well as ground gravity and magnetic datasets of the Swedish Geological Survey (SGU), have been compiled and analysed. This has been done using geophysical and petrophysical data in combination with geological information. Density and magnetic properties of rocks from the Tjårrojåkka area have been measured, with special attention given to the magnetic fabric of rocks and to its tectonic significance (Tarling and Hrouda, 1993; Borradaile and Henry, 1997). This modus operandi should give a basis for future geological, geophysical and structural studies in Tjårrojåkka.

The second task of this study is to test existing models for the IOCG deposits giving special attention to the following statements by Hitzman (2000): (1) IOCG deposits are structurally controlled; (2) Fe-oxides are abundant, while Fe-sulphides are almost absent in IOCG deposits; and (3) There is a spatial relationship between alterations (potassic) and Cu-deposits.

2. Geological setting and tectonic history

The area under investigation is located in northwestern Norrbotten, Sweden (Fig. 1), WSW of the city of Kiruna. The Archaean basement (>2.68 Ga) is overlain by Proterozoic rocks of Karelian (approx. 2.4–1.96 Ga) and Svecofennian (approx. 1.96–1.75 Ga) ages. The Karelian rocks (Kovo and Greenstone Groups) have been formed in a rift-related tectonic setting (Martinsson, 1997) and are overlain by Svecofennian supracrustal rocks. The Palaeoproterozoic supracrustal rocks underwent deformation and metamorphism during the Svecofennian orogeny (1.96–1.75 Ga).

The first component of the Svecofennian supracrustal rocks (Porphyrite Group) is composed of metamorphosed low-Ti andesites, basalts and some intercalations of felsic tufitic rocks. The calc-alkaline chemistry of these rocks suggests a compressional tectonic setting of formation. The Porphyry Group, younger than the Porphyrite Group, is formed by metamorphosed high-Ti basalts, minor trachyandesites and rhyolites. Southwest of the city of Kiruna, a minimum thickness of 4 km is reported for this

Fig. 1. Geological-tectonic map and simplified stratigraphic column (modified from SGU Northern Norrbotten Exploration Package and from Bergman et al., 2001; Swedish National Coordinate system RT90). Two major ductile deformation zones trending approximately NW–SE characterise the tectonic setting. Faults related to them and striking E–W seem to be spatially related to Fe and Cu occurrences, which are hosted by Svecofennian/Karelian supracrustal rocks. In the frame the area of Tjårrojåkka, target for the present study.

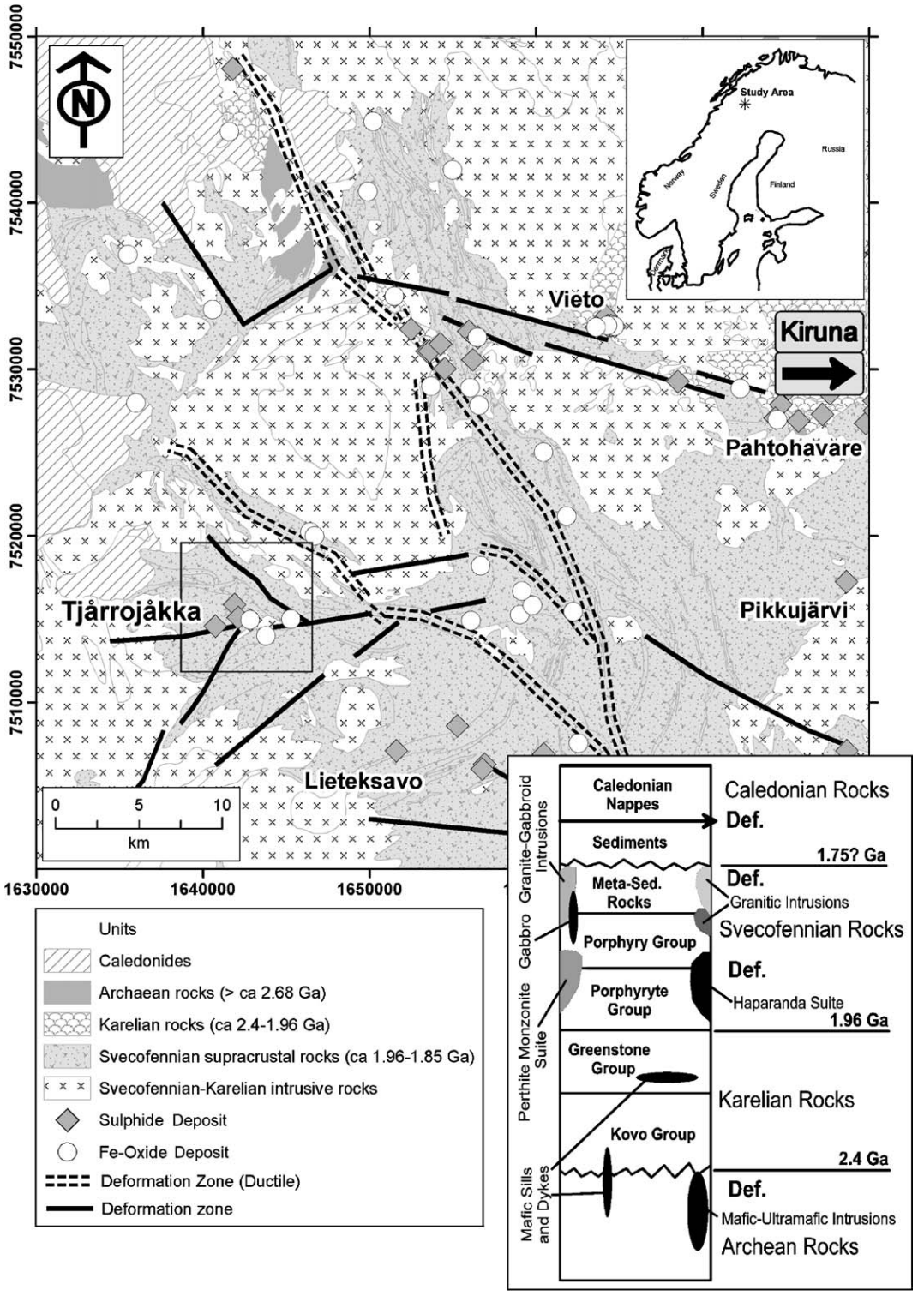
7550000
7540000
7530000
7520000
7510000
1630000
1640000
1650000
N
Study Area
Russia
Norway
Sweden
Finland
Vieto
Kiruna
Pahtohavare
Tjårrojåkka
Pikkujärvi
Lieteksavo
0
5
10
km
Units
Caledonides
Archaean rocks (> ca 2.68 Ga)
Karelian rocks (ca 2.4-1.96 Ga)
Svecofennian supracrustal rocks (ca 1.96-1.85 Ga)
Svecofennian-Karelian intrusive rocks
Sulphide Deposit
Fe-Oxide Deposit
Deformation Zone (Ductile)
Deformation zone
Caledonian Nappes
Sediments
Meta-Sed. Rocks
Porphyry Group
Porphyryte Group
Greenstone Group
Kovo Group
Granite-Gabbroid Intrusions
Gabbro
Perthite Monzonite Suite
Mafic Sills and Dykes
Caledonian Rocks
Def.
1.75? Ga
Def.
Granitic Intrusions
Svecofennian Rocks
Def.
Haparanda Suite
1.96 Ga
Karelian Rocks
2.4 Ga
Def.
Mafic-Ultramafic Intrusions
Archean Rocks

group. Its more alkaline character is typical of extensional tectonic environments (Bergman et al., 2001).

Different suits of intrusive rocks were formed simultaneously with the orogenetic event. The Haparanda suite is present mostly in the easternmost areas of northern Norrbotten and is composed of a wide set of rocks: from gabbros and diorites, to monzonites–monzodiorites, granodiorites and sometimes granites. The chemistry spans from alkali-calcic to calc-alkaline. The Perthite–monzonite suite is dominant in the area, with monzonites and quartz-monzonites formed around 1.88–1.86 Ga (Bergman et al., 2001). Some gabbroic intrusions may be associated with the Perthite–monzonite suite and these normally occur at the boundaries of the monzogranitic intrusions. Syn/post collisional plutonic rocks represent the subsequent stage of the intrusive events that affected the area. Granite–pegmatite association (Lina granites) has an age of 1.81–1.78 Ga (Bergman et al., 2001). Pegmatites, sometimes of large volume, are often associated with the predominant monzogranites. Deformation and metamorphism may have taken place at this time (Bergman et al., 2001).

The succession of the tectonic events began with a phase of extension and rifting of the Archaean crust in the early Proterozoic. With the orogenesis that followed the rifting, the previously formed continental/island arcs collided with the Archaean craton in a subduction-related tectonic setting. Around 1.93 Ga, south-westward subduction began below the rifted continent (Juhlin et al., 2002). Between 1.93 and 1.87 Ga, new continental crust was created together with the Svecofennian volcanic-belts (Gaal and Gorbatschev, 1987; Mellqvist et al., 1999). During the collision, metasedimentary and volcanic rocks were deformed by compression between different crustal blocks (Korja et al., 1993; Juhlin et al., 2002). A subsequent new collision of an arc or microcontinent caused the thrust over the Archaean craton (Juhlin et al., 2002).

During the second stage (1.86–1.75 Ga) deformations in a dextral transpressive system resulted in a probable E–W to NE–SW shortening. Consequently, partial thrusting of the accretionary prism and incompetent supracrustal belts onto the Archaean continental crust occurred (Gaal and Gorbatschev, 1987; Nironen, 1997; Mellqvist et al., 1999; Bergman et al., 2001). Magmatic and tectonic activity during the Svecofennian orogenetic event is believed to have favoured hydrothermal alteration together with the deposition of ore deposits (Bergman et al., 2001), which seem to be spatially related to major deformation zones. Finally, the crust was thinned along E–W striking zones by removing the lower crust during an extensional period characterised by anorogenic magmatism (1.6–1.5 Ga; Korja et al., 1993).

3. Tjårrojåkka geology and mineral deposits

In the Tjårrojåkka area, Svecofennian mafic to intermediate volcanic rocks are metamorphosed at low amphibolite facies (Bergman et al., 2001). Andesites are present in the central part of the investigated area, while basalts have been noted in the SW and NE. The basalts stratigraphically overlie the andesites (Edfelt and Martinsson, 2003). Several types of intrusions occur in the area. Metamorphosed dykes of mafic to intermediate character intrude the andesites; gabbroic intrusions have been found in the NE. The central area is also characterised by two distinct intrusions of gabbroic–dioritic and quartz-monzodioritic nature. A strong scapolitic alteration affected the metadiabases and basalts and is accompanied by the presence of biotite. K-feldspar alteration caused potassium enrichment in the andesites. This potassic alteration seems to be related to deformation zones and to Cu-occurrences (Bergman et al., 2001; Edfelt and Martinsson, 2003).

Various sub-economic Cu and Fe deposits occur in Tjårrojåkka. Some low-grade occurrences have been found in outcrop or as a boulder. A major Fe-deposit is located within the andesites in the centre of the area. This is a blind sub-economic ore with its top situated immediately below the bedrock surface and reaching a depth of 450 m. It is estimated to contain ~52.6 Mt of iron ore at 51.4% Fe (Bergman et al., 2001). The orebody can be described as a core of massive magnetite (60–67% Fe with 0.5 to 1.3% P) surrounded by a mineralised breccia (25–40% Fe and 0.4 to 3% P). Cu-sulphides can be found as low-grade disseminations in the wallrock (Edfelt and Martinsson, 2003).

The largest Cu-deposit in Tjårrojåkka is found approximately 1 km WNW of the Tjårrojåkka–Fe

deposit. The estimated tonnage of this 650 m long and 10 to 60 m wide body is 3.23 Mt of ore with 0.87% Cu, cut-off grade of 0.4% (Frietsch, 1997). The ore minerals are chalcopyrite and bornite in disseminations and veinlets. Other minerals are pyrite, magnetite, apatite, actinolite and minor haematite, chalcocite, covellite and traces of gold. The host rock is an altered andesite cut by metadiabases (Frietsch, 1997; Edfelt and Martinsson, 2003).

4. Petrophysical sampling and laboratory analyses

The sampling sites were selected with reference to a preliminary tectonic analysis of geophysical data and after geological investigations. Samples were collected along a line that intersects the major deformation zones (Fig. 2) using a portable drilling machine and oriented by sun and magnetic compasses; four to ten samples were collected at each site. One specimen for each sample has been used for the petrophysical studies. The specimen has a cylindrical shape, with a base diameter of 24 mm and a height of ~21 mm. All the rock types present in Tjårrojåkka have been sampled to obtain their density and magnetic properties. Petrophysical measurements

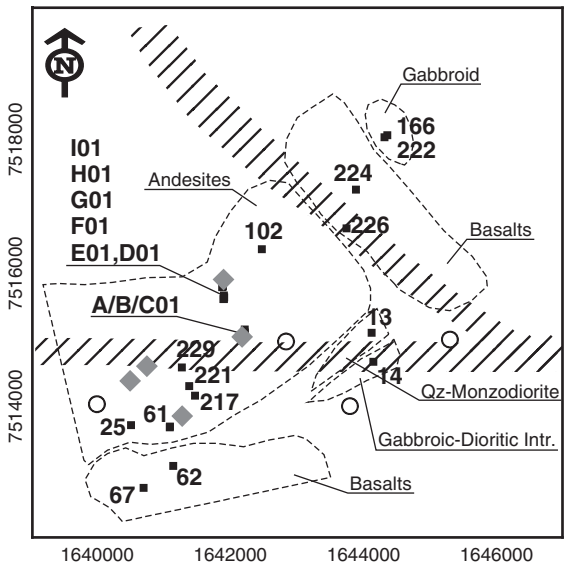

Fig. 2. Simplified geological map showing the positions of sampling sites (black squares), mineral occurrences (Cu = diamond; Fe = circle), deformation zones (hatched areas) and rock types.

have been performed at the laboratory of Division of Applied Geophysics of LTU (Luleå University of Technology). Specimen density has been obtained weighting the dry and water saturated specimens in water and in air.

Various magnetic properties were measured on the specimens. Intensity of natural remanent magnetisation (NRM) has been obtained for each specimen using a DC-SQUID magnetometer (2G-Enterprises). The same instrument was used for alternating field (AF) demagnetisation of few selected specimens. Bulk magnetic susceptibility and anisotropy of magnetic susceptibility (AMS) were measured using a Kappabridge KLY-3S (Geofyzika Brno, now AGICO Inc.). A furnace CS-3 of the same manufacturer was used for the measurement of the variation of magnetic susceptibility with temperature.

The magnetic fabric of each specimen is characterised by its AMS (Tarling and Hrouda, 1993). The AMS can be described as a 3×3 symmetric tensor and can be visualised as an ellipsoid whose major axis corresponds to the maximum magnetic susceptibility (K_{max}), the intermediate axis to the intermediate susceptibility (K_{int}) and the minimum axis to the minimum susceptibility (K_{min}).

The degree of anisotropy is expressed by Jelinek's (1981) corrected degree of anisotropy (P'):

$$P' = \exp\left\{2\left[(n_{max}-n)^2+(n_{int}-n)^2+(n_{min}-n)^2\right]\right\}^{1/2}$$

where $n=\frac{n_{max}+n_{int}+n_{min}}{3}$ and $n_i=\ln(K_i)$.

The shape of the AMS ellipsoid is characterised by the shape parameter T, which for $-1<T<0$ defines a prolate ('cigar-shaped') ellipsoid, while for $0<T<1$ identifies an oblate ("disk-shaped") AMS ellipsoid (Jelinek, 1981).

5. Geophysical datasets

Various geophysical databases have been analysed from a qualitative point of view. All the datasets have been obtained from SGU (Uppsala/Malå). Aeromagnetic data have been collected by the LKAB Company during the 1980s. The accuracy of the data is in the order of 2 nT. The flight clearance is 30 m, the line

separation 200 m (south–north direction) and the distance between the measuring points is ~40 m. The magnetic anomaly is given in reference to the Definite International Geomagnetic reference field 1965 (DGRF-65). Aeromagnetic data for the Tjårrojåkka area have been interpolated to a 50×50 m grid. Due to the high latitude of the area investigated, no reduction to the pole has been applied.

The airborne very low frequency EM-data (VLF) and airborne radiometric data have been collected by LKAB Company. The line distance is 200 m, clearance 30 m and point spacing 35 m. Direction of flight is south–north and for the positioning a Doppler system with auxiliary radar was used. VLF data have been collected using a Geonics EM18 and the transmitter was the GBR 16.0 kHz antenna in Rugby (UK). In the dataset the real part of the vertical magnetic field is given as a percentage of the horizontal magnetic field ($\mathrm{Re}[H_v]/H_o$).

Concentrations of potassium, U and Th are calculated from total radiometric spectra. Potassium concentration is given in percent while U and Th concentrations are given in parts per million.

The SGU gravity database in the Tjårrojåkka area consists of 71 measurements with variable station coverage (0.9 stations/km^2). Bouguer anomaly is given in reference to the International Gravity Standardisation Network 1971 (IGSN-71).

Ground magnetic measurements were collected in the 1960s and analog data have been manually digitised by the authors. The dataset presented in this study is a detail of the complete dataset and it is centred on major Fe-deposit in Tjårrojåkka. It represents the vertical magnetic field in nanoteslas (10×20 m station spacing).

6. Geophysical results

The outcrops in Tjårrojåkka are sparse and normally of limited extent. Therefore geophysical data analysis is crucial for the definition of tectonic elements. In the map of aeromagnetic data (Fig. 3a), a zone of low magnetic field characterises the NE segment of the area. A similar magnetic signature may be seen at regional scale a few kilometers towards NE in an area domi-

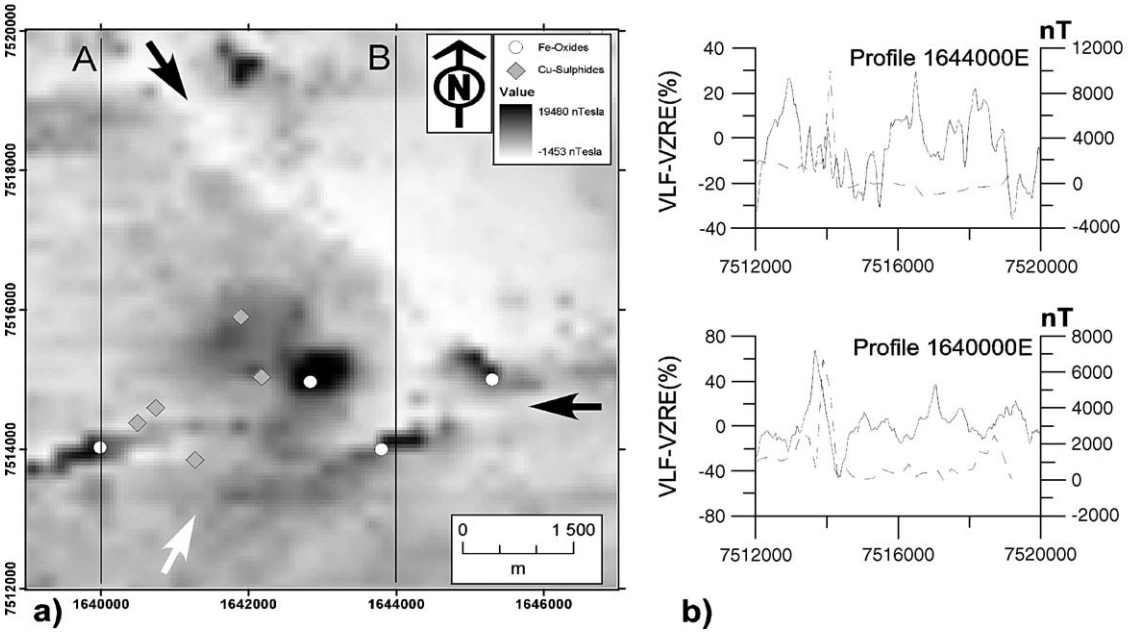

Fig. 3. (a) Aeromagnetic total field anomaly map and profiles (A–B) along which magnetic and VLF data are shown in (b). The white arrow indicates a probable post-glacial fault, while black arrows indicate low-magnetic lineaments interpreted as deformation zones. (b) Magnetic data (hatched lines) and VLF data (thick lines) are shown along the two profiles A and B. VLF data presented are the real part of vertical magnetic field as a percentage of the horizontal magnetic field.

nated by a granitic intrusion (Bergman et al., 2000). A linear feature striking NW–SE separates the NE zone from the centre of the area, where a general increase in the magnetic field, close to the major Fe-deposit (approximately 1643000E, 7515000N), appears to surround two Cu-occurrences.

High magnetic anomalies (>6000 nT) perfectly match with Fe-occurrences (magnetite). The E–W strike direction of one of these mineralised bodies (approximately 1643900E, 7514000 N) coincides with the strike expressed in ground gravity data (not presented here), supporting the interpretation that the mineralised body has an elongation axis in the E–W direction. The highly magnetic body in the SW has a strike that is approximately WSW–ENE and its continuation towards ENE shows a gentle change of strike to a pure E–W direction. A linear trend in aeromagnetic data (white arrow on Fig. 3a) striking SSW–NNE interrupts the continuity of other magnetic lineaments and it coincides with a post-glacial subvertical fault, visible in the field.

In fracture zones, circulating oxidising fluids can induce alteration in the rocks (Airo, 2002). This alteration may affect the ferromagnetic minerals (magnetite) and oxidise them to less magnetic minerals (e.g., haematite). Therefore linear low magnetic features may be interpreted as deformation zones (black arrows in Fig. 3a). The NW–SE striking lineament resembles the trend of the major sub-regional deformation zones (Fig. 1). The E–W striking lineament has been investigated through a combined magnetic/VLF analysis (Fig. 3b). In the profile 1640000E a peak in the magnetic anomaly is visible at 7514000N (~7000 nT) and corresponds to the *crossover* in the VLF data. As the flight direction is S–N, the asymmetric shape of the VLF signal ($\mathrm{Re}[H_v]/H_o$, E polarisation) suggests the presence of a subvertical conductor (McNeill and Labson, 1991), i.e., magnetite occurrence. In the profile 1644000E, a magnetic maximum is centred on the Fe-deposit, but it is not accompanied by a unique VLF anomaly. On the contrary there is a sequence of smaller VLF maximum and minimum anomalies, which are interpreted as a succession of subvertical conductors. They may be the expression of a wide fracture zone characterised by water-bearing fractures, with a consequent decrease in resistivity. The latter zone extends approximately from 7513400N to 7515000N.

Other conductive zones can be seen in the same profile at the points ~7515500N, 7516600N, 7517900N and 7519000N. The VLF anomaly at 7516600N matches with the NW–SE striking lineament defined from magnetic data, while the others can be expressions of minor fracturing areas bordering intrusive bodies (compare with position of quartz-monzodiorite and gabbro-diorite intrusions in Fig. 2). In Fig. 4b, VLF data have been plotted as a contour map and points of transition between high and low anomalies (conductive zones) seem to form linear trends striking basically SW–NE with a deflection towards E in the central areas. A different trend (NW–SE) can be noted in the NE, but it is fairly discontinuous and difficult to interpret because of its orthogonality to the direction of propagation of the VLF wave (McNeill and Labson, 1991).

Airborne radiometric data have been proven as a useful tool for geological mapping and for detection of alteration zones (Airo, 2002). The calculated K concentration has been used to define an approximate boundary for andesitic rocks (higher K content compared to basaltic rocks). A 3% calculated K content (Fig. 4a) has been chosen to define this boundary, as the alteration that affected the area in some cases increased the K content of andesite to values even higher than 4% (Bergman et al., 2001). K/Th ratios (K in %, Th in ppm) have been calculated to mark areas that suffered potassic alteration (Smith, 2002). In environments where the Quaternary cover is important, the interpretation of the radiometric data should be guided by analysis of topography, outcropping areas and response in measurements. In the Tjårrojåkka area, no relationship has been noted between the topographical highs and high values of K/Th. In the K/Th plot (Fig. 4a) there are several expressions of strong potassic alteration ($6<K/Th<10$), occurring almost exclusively within the highly potassic rock (andesite). Other minor enrichments in potassium can be detected within the basaltic rock ($4<K/Th<6$). More interestingly the K/Th anomalies seem to be spatially related to the Cu occurrences (compare maps in Figs. 3 and 4) and they also seem to mark a WSW–ENE trend. It suggests that potassic alteration follows the same approximate trend as that of the major mineralised bodies (both Cu- and Fe-) and that this kind of alteration may be related to the tectonic event,

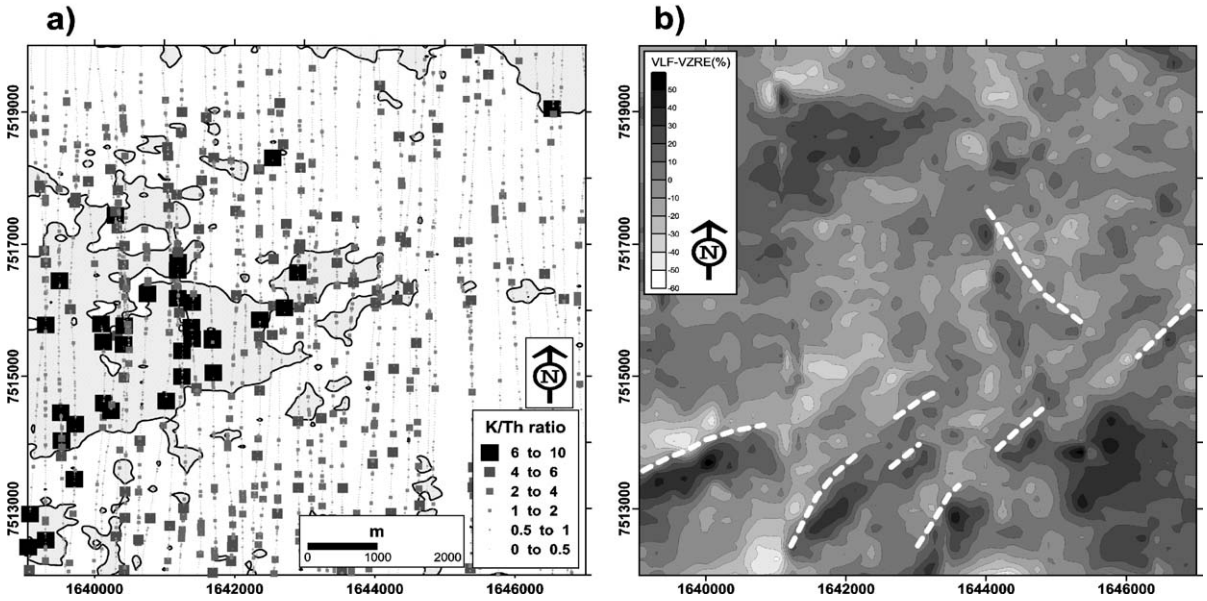

Fig. 4. (a) Map of the airborne radiometric data. The grey area marks the area of >3% of calculated potassium content. The high concentration of potassium in the extreme NE is due to the presence of an intrusion of granitic character. The size and colour of the square is proportional to the K/Th ratio and gives an estimate of the potassic alteration. (b) Map of the VLF data (real part of the vertical field as percentage of the horizontal field). The white hatched lines mark interpreted conductive zones.

which probably controlled the formation of the deposits themselves.

7. Petrophysics

Sites 62, 67, 224 and 226 are basalts with low to extremely high contents of magnetite. Amphibole is the major mineral with scapolite, K-feldspar and epidote as alteration minerals. Generally the sampled andesites comprise plagioclase phenocrysts, amphiboles and various alteration minerals as K-feldspars and, less commonly, scapolite. Some Cu-sulphides have been noted in samples from sites A01, B01 and C01; magnetite is also present. Samples from site B01 show an intense E–W cleavage. The gabbroic–dioritic rocks can be divided into two different groups. Sites 166 and 222 are characterised by the presence of amphiboles, plagioclase and minor K-feldspars (probably an alteration product). Site 14 is a mafic intrusion, gabbroic–dioritic in character, which suffered an intense potassic alteration. Cu-sulphides have also been noted in this intrusion (Edfelt and Martinsson, 2003). Site 13 is a quartz-monzodiorite with plagioclase, K-feldspars, amphiboles, biotite and quartz. Some mafic to intermediate dykes have been sampled in the central area. The strong scapolitic alteration affecting the rock does not allow a definitive classification of the rock and chemical analyses are strongly required. Preliminary data (Edfelt, personal communication, 2003) from sites D01, F01 and I01 indicate an intermediate character, while a mafic nature can be ascribed to site G01.

7.1. Density and magnetic properties

Magnetic susceptibility has been measured on 152 specimens from 24 outcrops. The histogram in Fig. 5 shows the susceptibility having a log-normal distribution. Anomalous high values (1.0–4.0 SI) are mostly due to the magnetite-enriched specimens from outcrops 62 and 67, which present a mean susceptibility of 1.23 SI and 2.31 SI, respectively. These data give an estimated magnetite content for these two sites of >10 wt.% (Tarling and Hrouda, 1993).

The high content of ferromagnetic minerals (l.s.) is clearly indicated in the diagram of susceptibility vs. density data (Fig. 6). Most of the site susceptibility

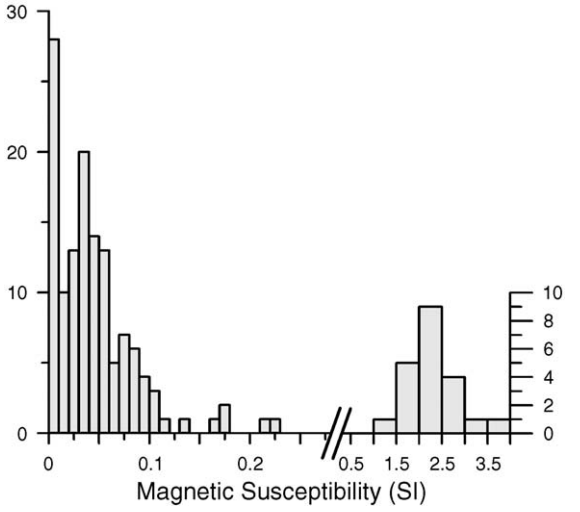

Fig. 5. Histogram of magnetic susceptibility. Note the anomalous peak at high magnetic susceptibilities (ca. 2.0 SI) and the low values at low susceptibilities (ca. 0.015 SI).

means fall within the ferromagnetic trend (the 'magnetite trend' of Henkel, 1991). Gabbroic (sites 14, 166 and 222) and basaltic rocks (sites 224 and 226) show high densities, while the magnetic susceptibility is variable. Thermomagnetic measurements indicate that magnetite is almost absent in a specimen from site 224 and its magnetism is dominated by paramagnetic minerals (Fig. 7d). Analogous paramagnetic character has been observed only for sites B01 and 61b. Andesitic specimen Tj4802 from site 221 (Fig. 7a) indicates that magnetite (Curie temperature 575 °C) is the dominant magnetic mineral. After heating in air an unstable magnetic phase was destroyed resulting in a final decrease in susceptibility of ~30% of the initial value. The Curie/Neel temperature of haematite (~675 °C) is not easily detectable because of the absolute dominance of the high susceptibility of magnetite, which masks the signal of haematite in susceptibility vs. temperature curves. A similar character of the susceptibility vs. temperature diagram has been noted for specimen Tj7902 (site 62, basaltic; Fig. 7b). The 'hump' between 200 and 350 °C is here more pronounced and a tail after 580 to 620 °C indicates that (Ti)-haematite is present.

Specimen Tj10702 from site 13 (Fig. 7c) shows stable thermomagnetic behaviour for this quartz-monzodiorite. The Curie temperature indicates magnetite as the only ferromagnetic mineral. The absence of the 'hump' and the stability of the magnetic susceptibility after heating–cooling cycle indicate that the unstable phase is not present.

An estimation of the grain size of magnetite can be obtained from the Königsberger-ratio Q (Fig. 8; Table 1). It has been demonstrated that Q is <1 for multi-domain magnetite (Dunlop and Özdemir, 1997). Therefore only the andesitic rock from site E01 (Fig. 8), for which Q is ~1.86, may contain single-domain grains of magnetite. Specimens from other outcrops usually give Q values <1, indicating multi-domain character for magnetite. To test the results obtained by analysis of the Königsberger ratio, a few selected specimens have been demagnetised in alternating field (AF) to maximum AF peaks of 40–60 mT (Fig. 9). The specimens are from different sites and all show a 'quasi-exponential' decay of the normalised remanence. This behaviour is usual for multi-domain magnetite (Dunlop and Özdemir, 1997) and this conclusion is supported by the value of the median destructive field (MDF)<10 mT. The MDF is the demagnetising field necessary to halve the initial NRM. MDF<12 mT indicates multi-domain magnetite, while MDF>22 mT suggest single-domain mag-

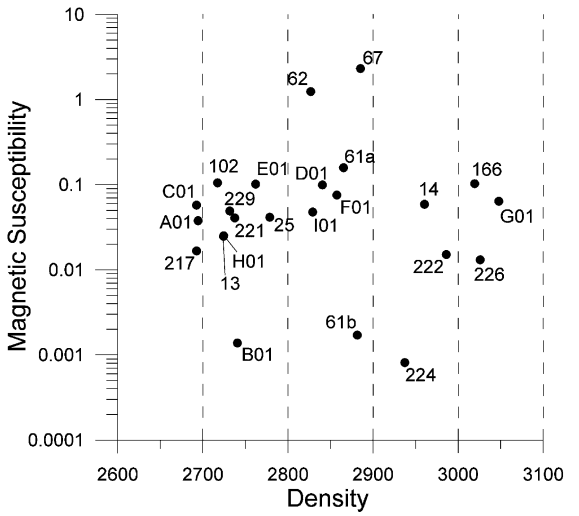

Fig. 6. Magnetic susceptibility vs. density diagram (SI units). Most of the site susceptibility-means fall in the ferromagnetic trend (Henkel, 1991). Paramagnetic minerals dominate in the rocks from sites B01, 61b and 224.

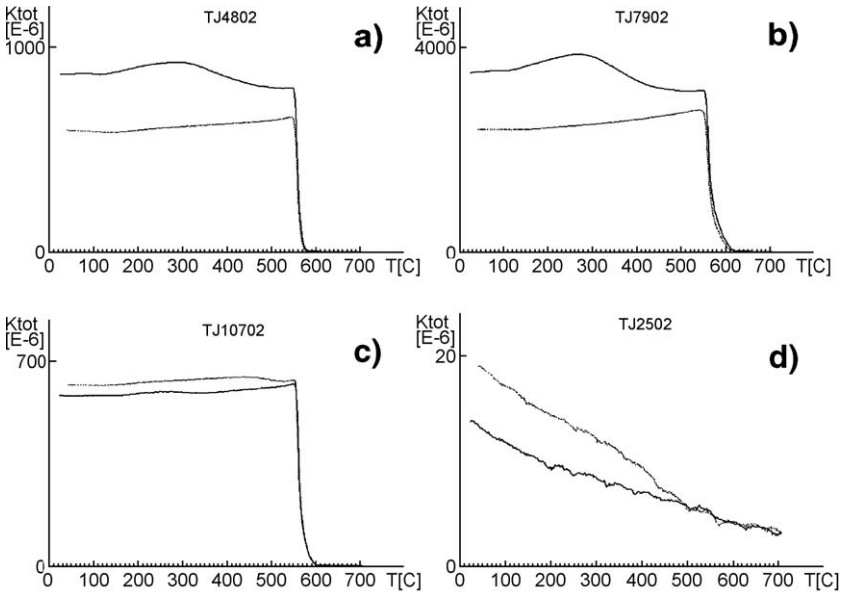

Fig. 7. Variation of magnetic susceptibility with temperature for four selected specimens. a) Andesitic rock (site 221). b) Basaltic rock (dominance of ferromagnetic minerals, site 62). c) Quartz-monzodiorite (site 13). d) Basaltic rock (dominance of paramagnetic minerals, site 224). Continuous line for heating curve and hatched line for cooling curve.

netite. If the MDF value is included between 12 and 22 mT the magnetite is of pseudo-single-domain character (Dunlop and Özdemir, 1997).

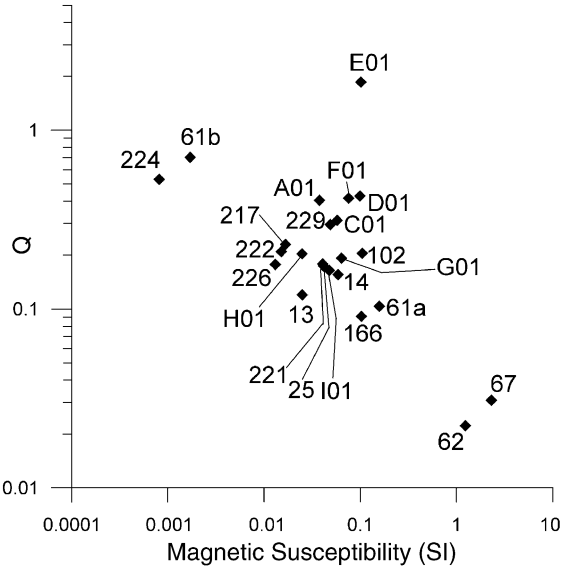

Fig. 8. Königsberger ratio Q vs. magnetic susceptibility diagram. The mean values of $Q<1$ indicate that multi-domain magnetite is dominant.

7.2. Magnetic fabric and anisotropy of magnetic susceptibility (AMS)

The distribution of the site means for the AMS parameters (P' = degree of AMS; T = shape parameter) indicate that the susceptibility ellipsoids are both prolate and oblate, with a slight dominance of oblate character (Fig. 10), while the degree of anisotropy varies from almost isotropic ($P'=1.02$ for site 14) to considerably anisotropic (few sites with $P'>1.4$; Fig. 10 and Table 2). No specific relationship has been noted between the parameters P', T and the rock type. Site mean directions for the K_{max}, K_{int} and K_{min} axes have been obtained from software based on statistics of Jelinek (1978).

It has been demonstrated in several works (e.g., Borradaile, 1987; Borradaile and Henry, 1997; Borradaile, 2001; Pares and van der Pluijm, 2002) that AMS directions may be related to finite strain directions and that there is a linear relationship between the natural strain and the logarithm of the degree of anisotropy ($\ln P'$; Tarling and Hrouda, 1993). If the magnetic susceptibility is >0.002 SI, the AMS is dominated by the ferromagnetic phase (Borradaile et al., 1998). In the case of magnetite, the AMS is

Table 1
Physical properties for various sites and rock types in Tjårrojåkka

Petrophysical properties									
Site	NRM (A/m)		K (SI)		Q		Dens. (kg/m^3)		Rock Type
	Geo. Mean		Geo. Mean		Geo. Mean		Avg.		
13	0.118	(4)	0.02498	(4)	0.120	(4)	2725	(4)	Quartz-monzodiorite
14	0.368	(9)	0.05866	(9)	0.156	(9)	2960	(9)	Gabbro–diorite
25	0.292	(8)	0.04134	(8)	0.174	(8)	2779	(8)	Andesite
61a	0.300	(4)	0.15746	(6)	0.103	(4)	2865	(6)	Andesite
61b	0.048	(7)	0.00170	(7)	0.704	(7)	2881	(7)	Andesite
62	1.002	(6)	1.23843	(7)	0.022	(6)	2827	(6)	Basalt
67	2.801	(6)	2.30956	(8)	0.031	(6)	2885	(4)	Basalt
102	0.871	(7)	0.10493	(7)	0.204	(7)	2717	(6)	Andesite
166	0.375	(6)	0.10274	(6)	0.091	(6)	3019	(6)	Gabbroid
217	0.154	(7)	0.01662	(7)	0.229	(7)	2693	(7)	Andesite
221	0.285	(7)	0.04055	(7)	0.178	(7)	2737	(7)	Andesite
222	0.127	(6)	0.01510	(6)	0.209	(6)	2986	(6)	Gabbroid
224	0.017	(7)	0.00081	(7)	0.530	(7)	2937	(8)	Basalt
226	0.093	(7)	0.01305	(7)	0.178	(7)	3026	(7)	Basalt
229	0.583	(8)	0.04892	(8)	0.297	(8)	2732	(8)	Andesite
A01	0.612	(5)	0.03764	(5)	0.404	(5)	2694	(5)	Andesite
B01			0.00138	(5)			2741	(5)	Andesite
C01	0.724	(6)	0.05746	(6)	0.313	(6)	2693	(6)	Andesite
D01	1.688	(5)	0.09918	(5)	0.428	(5)	2840	(5)	Dyke (andesitic)
E01	5.769	(3)	0.10129	(5)	1.856	(3)	2762	(3)	Andesite
F01	1.251	(6)	0.07537	(6)	0.417	(6)	2857	(6)	Dyke (mafic/andesitic)
G01	0.491	(5)	0.06370	(5)	0.192	(5)	3048	(5)	Dyke (mafic)
H01	0.210	(5)	0.02476	(6)	0.203	(5)	2724	(5)	Andesite
I01	0.407	(4)	0.04750	(5)	0.164	(4)	2829	(5)	Dyke (andesitic)

Note: Geometric mean has been calculated for the natural remanent magnetisation NRM, the magnetic susceptibility K and the Königsberger ratio Q, while arithmetic mean has been calculated for density. The number of specimens is given in brackets.

controlled by the shape of the grain and by the spatial distribution of the magnetite grains within the para-/dia-magnetic silicatic matrix (Tarling and Hrouda, 1993). For multi-domain magnetite the K_{max} direction is parallel to the maximal elongation of the grain (Tarling and Hrouda, 1993; Dunlop and Özdemir, 1997). Therefore the direction of the K_{max} may be interpreted as a magnetic lineation, while the K_{min} may be considered as a pole to the magnetic foliation plane (defined by the K_{max}–K_{int} plane). In Fig. 11, K_{min} and K_{max} directions have been plotted on stereograms. Site mean magnetic foliations F and lineations L lower than 5% (Table 2) have not been considered to have any tectonic significance; hence their K_{max} and K_{min} directions have been plotted (crosses) only to avoid loss of information.

Basaltic and gabbroic rocks in the NE part of the investigated area (sites 166, 222, 224 and 226; Fig. 2) show a magnetic lineation striking approximately 210°, with a dip of 30° to 45° (Table 3; Fig. 11). Their poles to the magnetic foliations have a strike of ~60° with a dip of ~45°. It can be noted that the axes of AMS for basalts are more clustered than those of the gabbroic intrusion. Sites in the NW part are of andesitic character (sites 102, E01, H01) and some others (D01, F01, G01 and I01) are dykes of intermediate to mafic nature that have intruded the andesites. In all these outcrops the magnetic foliation generally shows SW–NE strike, together with a subvertical magnetic lineation, especially developed in dyke D01. An exception is represented by mafic dyke G01, which shows a vertical magnetic lineation associated with a NW–SE striking magnetic foliation, indicating that this dyke probably intruded after the deformation. Sites A01, B01 and C01 are in proximity of the major Cu-deposit in the Tjårrojåkka area and presence of Cu-sulphides in these outcrops has been noted. AMS directions indicate that a subvertical

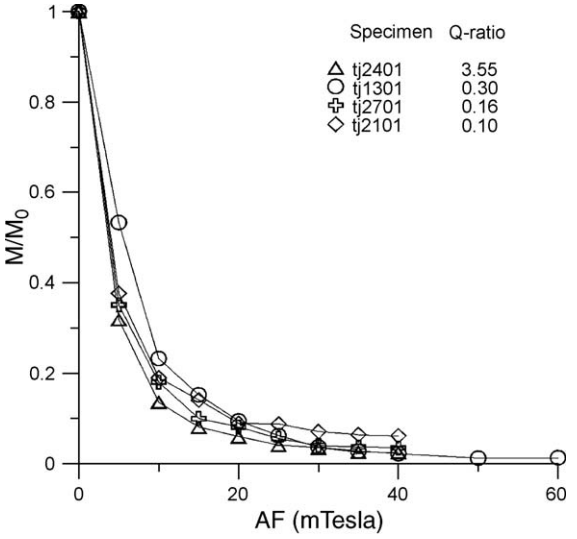

Fig. 9. Remanence behaviour during AF-demagnetisation of rocks with different values of Q. The median destructive field (MDF)<10 mTesla and the quasi-exponential decay indicate multi-domain magnetite as a dominant magnetic mineral.

magnetic lineation characterises these outcrops, while the magnetic foliation (not defined for site B01) is subvertical and striking approximately E–W. The same trends have been obtained for sites 219, 221, 25 and, with some differences, for site 217, which are located in the centre of the studied area. In these cases magnetic lineations and poles to the magnetic foliation planes are well grouped, giving a general subvertical magnetic lineation and E–W striking magnetic foliation. Outcrop 217 differs from the others with a N–S striking magnetic lineation (189°/63°) and K_{int} and K_{min} directions distributed within a plane perpendicular to the magnetic lineation. In the SW, both the andesitic and basaltic rocks (sites 61a/b and 62, 67, respectively) present intermediate to low degree of AMS with poorly defined principal directions of AMS. For sites 62 and 67, the K_{min} directions cluster at around 330°/20° (Table 3), while the K_{max} and K_{int} axes are scattered orthogonally to the K_{min}. This is also reflected in a foliated character of the shape parameter T (0.32 and 0.50, respectively). Site 61a/b cannot be used for tectonic interpretation because of the excessive scattering of the specimen AMS directions. A short description of the magnetic fabric for specimens from sites 13 and 14 is given in the discussion below.

Assuming that the lnP' is in linear relationship with natural strain, a plot of this variable may indicate

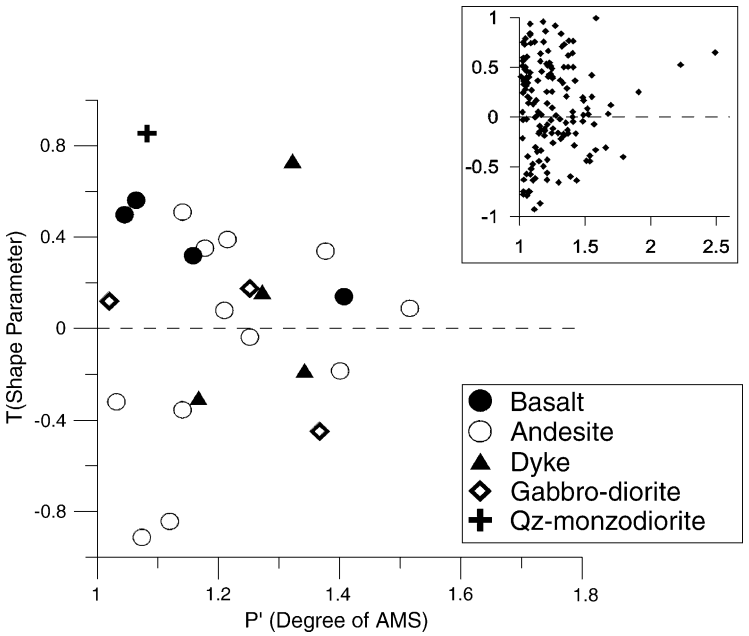

Fig. 10. T vs. P' diagram for different sites in Tjårrojåkka. In the inset the same diagram is shown for all the specimens.

Table 2
AMS parameters for the different sites in the area

Magnetic fabric parameters						
Site	N	K (SI) Geo. Mean	P'	L (K_{max}/K_{int})	F (K_{int}/K_{min})	T
13	4	0.02498	1.082	1.005	1.068	0.854
14	9	0.05866	1.020	1.009	1.011	0.120
25	8	0.04134	1.141	1.091	1.042	−0.356
61a	6	0.15746	1.141	1.032	1.100	0.509
61b	7	0.00170	1.032	1.021	1.011	−0.321
62	7	1.23843	1.158	1.050	1.100	0.319
67	8	2.30956	1.045	1.011	1.032	0.498
102	7	0.10493	1.252	1.124	1.114	−0.038
166	6	0.10274	1.252	1.096	1.140	0.175
217	7	0.01662	1.074	1.062	1.003	−0.914
221	7	0.04055	1.215	1.060	1.141	0.389
222	6	0.01510	1.367	1.245	1.087	−0.450
224	7	0.00081	1.064	1.013	1.047	0.561
226	7	0.01305	1.407	1.157	1.214	0.140
229	8	0.04892	1.178	1.054	1.115	0.351
A01	5	0.03764	1.401	1.220	1.146	−0.186
B01	5	0.00138	1.120	1.098	1.008	−0.844
C01	6	0.05746	1.377	1.110	1.234	0.338
D01	5	0.09918	1.342	1.191	1.125	−0.193
E01	5	0.10129	1.516	1.209	1.253	0.088
F01	6	0.07537	1.322	1.036	1.248	0.723
G01	5	0.06370	1.167	1.105	1.054	−0.313
H01	6	0.02476	1.210	1.092	1.108	0.079
I01	5	0.04750	1.272	1.107	1.148	0.150

Note: N is the number of specimens. K is the mean magnetic susceptibility. P', L, F and T parameters as defined by Jelinek (1981).

Table 3
Declination (D) and inclination (I) of the maximum and minimum axes of AMS ellipsoid

Site mean directions for K_{max} and K_{min}				
Site	$D \cdot K_{max}$	$I \cdot K_{max}$	$D \cdot K_{min}$	$I \cdot K_{min}$
13	119	64	210	0
14	21	5	279	70
25	159	81	357	8
61a	202	55	354	32
61b	195	63	4	27
62	186	78	326	10
67	101	50	339	25
102	205	52	357	35
166	220	33	57	56
217	189	63	313	16
221	258	48	357	8
222	209	23	101	37
224	227	42	65	47
226	211	42	66	42
229	262	44	5	13
A01	278	75	171	4
B01	206	80	28	10
C01	116	66	1	11
D01	195	83	310	3
E01	75	87	313	2
F01	211	72	329	9
G01	302	63	49	9
H01	230	77	121	4
I01	214	52	123	1

major strain differences in the area (Fig. 12a). High degree of AMS can be noted in the central and NE parts of the area. The directions of the K_{max}–K_{int} planes have also been plotted in Fig. 12a and as a Rose diagram (Fig. 12b). Only when a foliated character of the AMS is defined, can these planes be considered as magnetic foliation planes. Three major trends in directions can be seen from the Rose diagram: one is an E–W striking direction, which characterises the very central part of the area; another is a NW–SE direction identified in the NE part; and finally a SW–NE direction that characterises the outcrops in NW part of the central area. Note that the directions now defined match perfectly with linea-

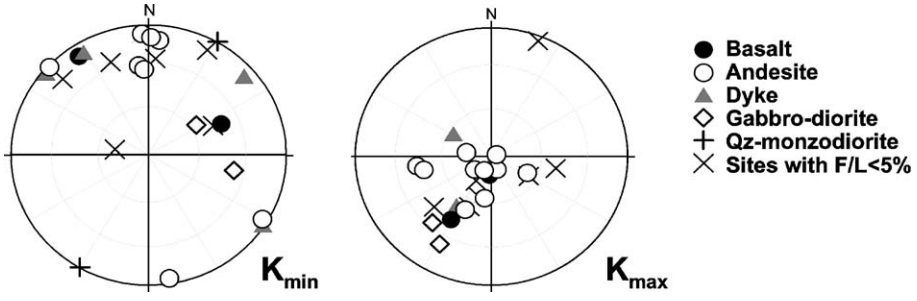

Fig. 11. Stereographic projections of the minimum (left) and maximum (right) axes of the AMS ellipsoid. X mark site mean directions when the lineation L or foliation F parameters ($F=K_{int}/K_{min}$; $L=K_{max}/K_{int}$) are <5%.

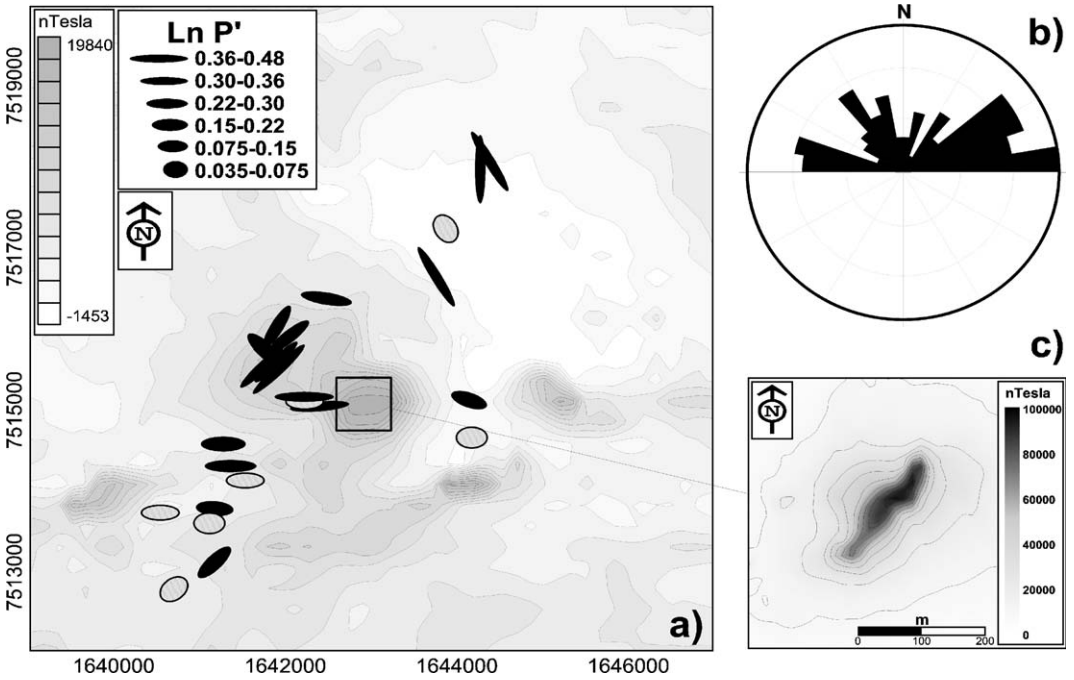

Fig. 12. (a) Magnetic anomaly map (total field), the directions of K_{max}–K_{int} plane (long axis of ellipses) and the logarithm of the degree of AMS (expressed by the eccentricity of the ellipses) are shown. Black ellipses for sites with a degree of foliation $F>5\%$, grey ellipses when $F<5\%$ ($F=K_{int}/K_{min}$). (b) Rose diagram for magnetic foliation directions. (c) Detailed map of the vertical magnetic field from the Tjårrojåkka-Fe deposit.

ments defined from the aeromagnetic data. In addition a detailed vertical magnetic field map centred on the major Fe-deposit indicates a SW–NE strike of the magnetic body that is parallel to the magnetic foliations in andesites and dykes in the NW. A probable E–W dextral deformation of the magnetic body can, however, be seen from ground magnetic data. Such an E–W deformation is also indicated by AMS data for sites in proximity of the orebody. Sites in the SW part of the area are characterised by low degrees of AMS and no well-defined AMS directions, but at least a generic SW–NE trend can be recognised for magnetic foliation in specimens from sites 62 and 67.

8. Discussion

The magnetic fabric can be of primary (syngenetic with the rock) or of secondary origin (Tarling and Hrouda, 1993). The latter is due to tectonism and metamorphic events and to recrystallisation phenomena. Because of the metamorphism that affected the area of Tjårrojåkka, and taking into account the presence of numerous zones of deformation, the AMS is expected to be generally of secondary origin. However, an exception may be demonstrated by the quartz-monzodiorite and by the dioritic–gabbroic intrusion (sites 13 and 14, respectively), for which the magnetic fabric may be primary.

Various mechanisms and models for rotation and deformation of AMS ellipsoids within and in proximity to deformation zones have been proposed, and a general conclusion is that in tectonic studies a one-to-one relationship exists between AMS directions and finite strain directions (e.g., Tarling and Hrouda, 1993; Borradaile and Henry, 1997; Borradaile et al., 1998). For multi-domain magnetite in a non-coaxial transpression, the grain elongations move towards the shear direction, while the K_{min} migrates into the plane containing the shear direction and the pole to the shear-plane. In shear zones and thrusts the AMS axes rotate towards the shear-plane (Borradaile and Henry, 1997). In cases of stress-controlled crystallisa-

tion or nucleation, neo-formed crystals align perfectly with the contemporary stress-field (Borradaile and Henry, 1997; Borradaile et al., 1999).

From geophysical data (airborne magnetics and ground gravity data; Fig. 13) three major trends can be defined. In the SW, a gradient trend in the Bouguer anomaly strikes SW–NE. In the same area, AMS directions (sites 62, 67 and, in minor part, site 61a/b) give a magnetic foliation with the same approximate strike and with a dip of ~70°SSE. These data suggest the possibility of a subvertical movement slightly directed towards NW. Site 25 presents a subvertical magnetic lineation associated with E–W striking magnetic foliation. Together with other sites in the central area (sites 217, 219, 221, 229, A01, B01, C01), the well-defined magnetic lineation is subvertical or dipping ~60°W in the easternmost outcrops. The magnetic foliation for specimens from these outcrops is invariably striking E–W. Outcrops in the NW part of the central area present vertical lineation with SW–NE magnetic foliation, which is parallel to the strike defined for the major Fe-deposit. In the NE, aeromagnetic, VLF, gravity data and magnetic foliation mark a different NW–SE trend. In this area the magnetic lineation dips ~30°SSW.

These observations may indicate that, in the central area, there was an original SW–NE structural trend, still visible in the central and south-western parts of the area, which has been overprinted by the E–W striking tectonic event. The original trend is also reflected by the shape of the mineralised body, the direction of which may suggest a preferential direction of crustal weakness. This is in good agreement with a model proposed by Wright (1988; Fig. 14), who interpreted an ESE–WNW thrust of supracrustal rocks from geological data, with subsequent ramping and development of vertical axial planar cleavage in the most incompetent rocks.

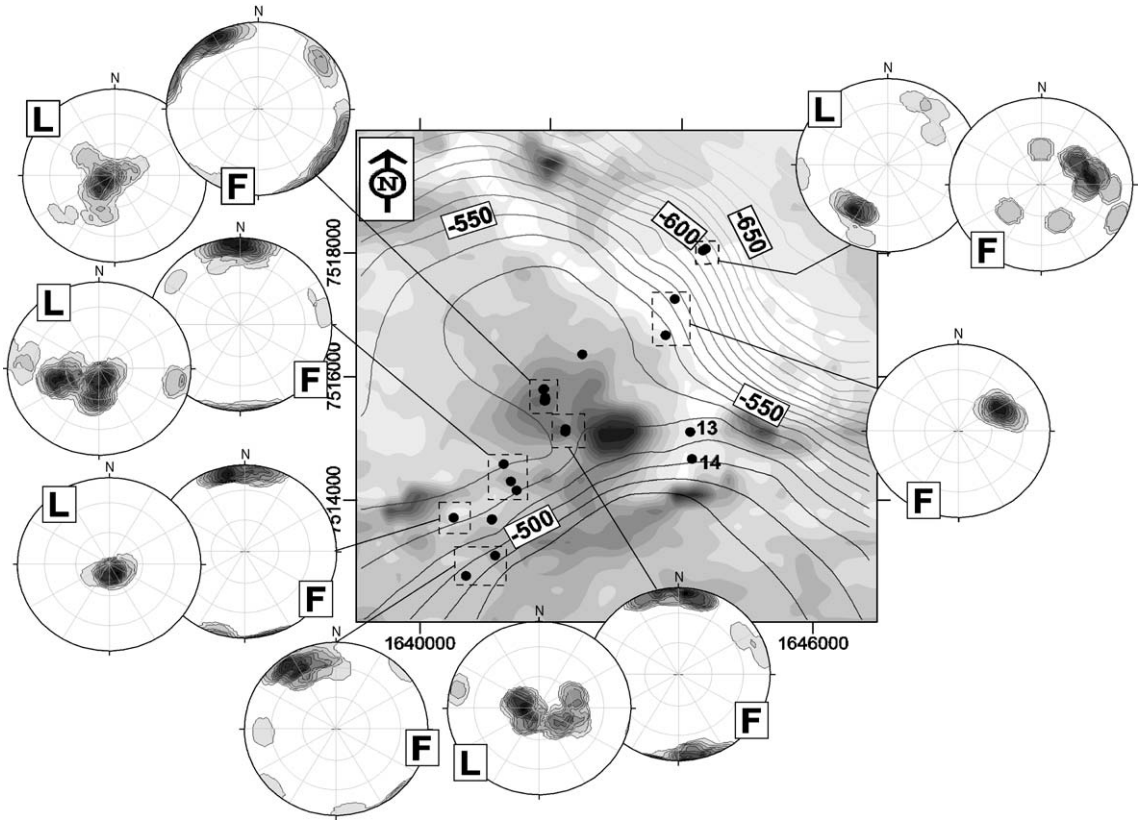

Fig. 13. Map of the total magnetic field anomaly (grey tones; black for high anomalies), gravity anomaly map (isolines; expressed in g.u.) and directions of magnetic foliation/lineation (*F*/*L*) shown in stereograms.

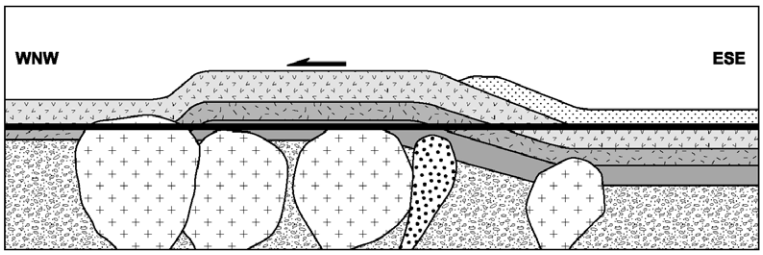

Fig. 14. Tectonic model for the Kiruna area (simplified from Wright, 1988). Thrust and folding of supracrustal units (in grey) toward WNW on the basement (white with grains) are shown. Subsequently several granitic (white with crosses) and gabbroic (black dots on white) plutons intruded the basement and the supracrustal units. Black line marks the present erosional level.

The E–W deformation zone is characterised by a magnetic lineation dipping from 90° to 60°W, which suggests a dextral shear character for the deformation.

In the NE, the AMS directions suggest a probable thrust of meta-volcanic rocks and gabbros towards NE. Magnetic fabric for site 224 and 226 is dominated by paramagnetic and ferromagnetic phases, respectively; however, they show the same AMS directions. If magnetite is secondary, it formed before or during this tectonic event or it may mimic the fabric of the pre-existing silicates. The deformation may have been controlled by the presence of a crustal discontinuity due to a granitoid intrusion in the northeast (Perthite–monzonite suite; Bergman et al., 2001), which is also indicated by the gravity data (Fig. 13). The strike direction of magnetic foliation for sites 224 and 226 is parallel to the direction of a regional ductile shear zone related to the granitoid itself (see Fig. 1). Poles to the magnetic foliation obtained for specimens from site 13 (quartz-monzodiorite; Fig. 15a) group at 210°/0°, giving a strike direction for the magnetic foliation that matches perfectly with the boundaries of the granitoid at regional scale. Unfortunately the size of the outcrop and its isolated location does not allow a better correlation with the major granitoid intrusion. However it can be noted that the Perthite–monzonite suite shows magmatic foliation near its margins (Bergman et al., 2001).

An open problem is represented by the specimens from the gabbroic rock of site 14. The long and intermediate axes of the AMS ellipsoid (Fig. 15b) are scattered within a subhorizontal plane, while the minimum axis roughly groups at ~280°/70°. In spite of some alteration of the rocks at sites 13 and 14, their magnetic fabric does not show the same trends shown by other rocks in the area. It may be due to a later emplacement of the intrusions after the major deformations, as proposed by Wright (1988). An alternative interpretation may be a peripheral location of both intrusive bodies in respect to the zones of major strain. This interpretation is supported, to some extent, by the fact that the magnetic foliation for site 14 is gently

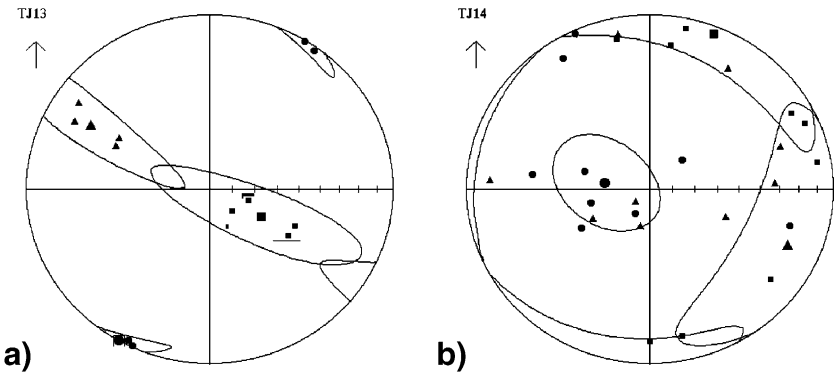

Fig. 15. (a) Directions of AMS ellipsoid axes from site 13. (b) Directions of AMS ellipsoid axes from site 14. Square for K_{max}, triangle for K_{int} and circle for K_{min}. Ellipses mark 95% confidence limit (Jelinek, 1978).

dipping towards ESE, which may be an effect of the ESE–WNW compression.

Analyses of the magnetic mineralogy show that multi-domain magnetite is the most common magnetic mineral in Tjårrojåkka. Specimens from volcanic rocks show a decrease of magnetic susceptibility after heating/cooling cycle in air. This behaviour indicates the presence of an unstable phase, which may be difficult to interpret.

The wide peak at 300 °C and the following drop at 320 to 350°C may be due to the presence of Ti-magnetite, which exsolves into a Ti-rich component and a Ti-poor magnetite around 300 °C (Dunlop and Özdemir, 1997; Jones et al., 2001). This magnetite oxidises to maghemite (metastable γFe_2O_3) that may invert irreversibly to stable and less magnetic haematite at ~350 °C (αFe_2O_3; Tarling and Hrouda, 1993), thus explaining the decrease in susceptibility after cooling. An alternative interpretation is that Ti-maghemite is original and not created during the laboratory procedure. This Ti-maghemite becomes instable during heating and exsolves into ilmenite–magnetite intergrowths (e.g., Lyons et al., 2002; Dunlop and Özdemir, 1997). Unfortunately the resulting intergrowths are in texture and composition very similar to those obtained when Ti-magnetite, with the same amount of Ti, undergoes oxidation.

The rocks are believed to be volcanics extruded into subaerial or submarine environments, where they may have been oxidised (Kontny et al., 2003; Matzka et al., 2003). This supports the thesis that the unstable phase may be oxidised Ti-magnetite (Ti-maghemite; Dunlop and Özdemir, 1997). Furthermore, hydrothermal alteration in the presence of ground- or seawater during low-grade metamorphism may induce oxidation of original Ti-magnetite in both subaerial and submarine lava flows (Dunlop and Özdemir, 1997).

9. Conclusions

In the region SW of the city of Kiruna and in the Tjårrojåkka area, Fe and Cu deposits occur in a complicated tectonic environment. Geophysical and petrophysical analyses allow the definition of various trends of tectonic deformation zones at both the local and regional scales. In Tjårrojåkka a SW–NE trend is shown by elongation of the major Fe-mineralised body and by the magnetic foliation plane in several outcrops approximately 1 km NW of the Fe-deposit. This, together with the epigenetic character of the deposits (Bergman et al., 2001), the spatial relationship between the Cu-, Fe-occurrences, potassic alteration and deformation zones, suggests a connection between the formation of the mineral deposits and a tectonic event. The tectonic event may be related to an ESE–WNW regional compression in the Kiruna area and westwards, as has been proposed by other authors (e.g., Wright, 1988). After the formation of the Fe–deposit, an E–W striking deformation affected the central and western areas. Magnetic foliation and magnetic lineation directions suggest a dextral transpressive character for this deformation. Such an E–W deformation is also indicated by lineaments in the airborne magnetic and VLF maps, lineaments that trend SW–NE in the south and gently change their directions to almost pure E–W in the centre of the area. In the NE part a probable thrust involving volcanics and gabbros is suggested. The movement of this thrust seems to be directed from SW towards NE. The thrust may have been controlled by the presence of a massive granitic body, whose boundary trends NW–SE, also at regional scale. The same trend has been found for the magnetic foliation in an outcrop that is probably related to that granitic intrusion.

Airborne radiometric data have been demonstrated to be a useful method for mapping boundaries between rocks with different K contents (e.g., andesites and basalts). In addition the ratio K/Th has also indicated areas affected by potassic alteration, which here seem to be spatially related with Cu-deposits.

Petrophysical analyses indicate that Fe-oxides are widely present at Tjårrojåkka, whereas Fe-sulphides are almost absent. This is in perfect agreement with the IOCG character of the deposits. Among the Fe-oxides, magnetite seems to be dominant. A thermomagnetically unstable phase has been noted, particularly in volcanic rocks, and it is suggested to be (Ti)-maghemite resulting from oxidation of (Ti)-magnetite in a subaerial/marine environment or during hydrothermal activity related to metamorphism.

Acknowledgements

Malå Georange and LTU financed this project. Phelps-Dodge Ltd. is acknowledged for logistic sup-

port and for permission to publish this contribution. The authors wish to thank Roger Lindfors for help during the field and laboratory work, Milan Vnuk for drawing some pictures and Åsa Edfelt for providing helpful geological information. The suggestions of Nigel Phillips, an anonymous reviewer and Chief Editor Nigel J. Cook greatly improved the original manuscript.

References

Airo, M.-L., 2002. Aeromagnetic and aeroradiometric response to hydrothermal alteration. Surveys in Geophysics 23, 273–302.

Bergman, S., Kübler, L., Martinsson, O., 2000. Regional geological and geophysical maps of northern Norrbotten county: magnetic total field map. Sveriges Geologiske Undersökning, Ba 56, 4.

Bergman, S., Kübler, L., Martinsson, O., 2001. Description of regional geological and geophysical maps of northern Norrbotten County (east of the Caledonian orogen). Sveriges Geologiske Undersökning, Ba 56 (110 pp.).

Borradaile, G.J., 1987. Anisotropy of magnetic susceptibility: rock composition versus strain. Tectonophysics 138, 327–329.

Borradaile, G.J., 2001. Magnetic fabrics and petrofabrics: their orientation distributions and anisotropies. Journal of Structural Geology 23, 1581–1596.

Borradaile, G.J., Henry, B., 1997. Tectonic applications of magnetic susceptibility and its anisotropy. Earth-Science Reviews 42, 49–93.

Borradaile, G.J., Lagroix, F., King, D., 1998. Titling and transpression of an Archaean anorthosite in northern Ontario. Tectonophysics 293, 239–254.

Borradaile, G.J., Werner, T., Lagroix, F., 1999. Magnetic fabrics and anisotropy-controlled thrusting in the Kapuskasing Structural Zone, Canada. Tectonophysics 302, 241–256.

Dunlop, D.J., Özdemir, Ö., 1997. Rock Magnetism — Fundamentals and Frontiers. Cambridge University Press, Cambridge, U.K. 573 pp.

Edfelt, Å., Martinsson, O., 2003. The Tjårrojåkka Fe-oxide Cu (–Au) occurrence, Kiruna area, northern Sweden. In: Eliopoulos, D.G., et al., (Eds.), Mineral Exploration and Sustainable Development. Millpress, Rotterdam, pp. 1069–1071.

Frietsch, R., 1997. The iron ore inventory programme 1963–1972 in Norrbotten County. Sveriges Geologiske Undersökning, Rapport 92 (77 pp.).

Gaal, G., Gorbatschev, R., 1987. An outline of the Precambrian evolution of the Baltic Shield. Precambrian Research 35, 15–52.

Henkel, H., 1991. Petrophysical properties (density and magnetization) of rocks from the northern part of the Baltic Shield. Tectonophysics 192, 1–19.

Hitzman, M.W., 2000. Iron oxide–Cu–Au deposits: what, where, when and why. In: Porter, T.M. (Ed.), Hydrothermal Iron Oxide Copper–Gold and Related Deposits: A Global Perspective, vol. 1. Australian Mineral Foundation, Adelaide, pp. 9–25.

Hitzman, M.W., Oreskes, N., Einaudi, M.T., 1992. Geological characteristics and tectonic setting of Proterozoic iron oxide (Cu–U–Au–REE) deposits. Precambrian Research 58, 241–287.

Jelinek, V., 1978. Statistical processing of anisotropy of magnetic susceptibility measured on groups of specimens. Studia Geophysica et Geodaetica 22, 50–62.

Jelinek, V., 1981. Characterization of the magnetic fabric of rocks. Tectonophysics 79, 63–67.

Jones, D.L., Duncan, R.A., Briden, J.C., Randall, D.E., MacNiocaill, 2001. Age of the Batoka basalts, northern Zimbabwe, and the duration of Karoo Large Igneous Province magmatism. Geochemistry Geophysics Geosystems, AGU 2 (2) (paper 2000GC000110).

Juhlin, C., Elming, S.-Å., Mellqvist, C., Öhlander, B., Weihed, P., Wikström, A., 2002. Crustal reflectivity near the Archaean–Proterozoic boundary in northern Sweden and implications for the tectonic evolution of the area. Geophysical Journal International 150, 180–197.

Kontny, A., Vahle, C., de Wall, H., 2003. Characteristic magnetic behavior of subaerial and submarine lava units from the Hawaiian Scientific Drilling Project (HSDP-2). Geochemistry Geophysics Geosystems, AGU 4 (2) (paper 2002GC000304).

Korja, A., Korja, T., Luosto, U., Heikkinen, P., 1993. Seismic and geoelectric evidence for collisional and extensional events in the Fennoscandian Shield — implications for Precambrian crustal evolution. Tectonophysics 219, 129–152.

Lyons, J.J., Coe, R.S., Zhao, X., Renne, P.R., Kazansky, A.Y., Izokh, A.E., Kungurtsev, L.V., Mitrokhin, D.V., 2002. Paleomagnetism of the early Triassic Semeitau igneous series, eastern Kazakstan. Journal of Geophysical Research 107 (B7). doi: 10.1029/2001JB000521.

Martinsson, O., 1997. Tectonic setting and metallogeny of the Kiruna Greenstones. Ph.D. thesis, Luleå University of Technology, Sweden, 1997:19, 162 pp.

Matzka, J., Krasa, D., Kunzman, T., Schult, A., Petersen, N., 2003. Magnetic state of 10–40 Ma old ocean basalts and its implications for natural remanent magnetization. Earth and Planetary Science Letters 206, 541–553.

McNeill, J.D., Labson, V.F., 1991. Geological mapping using VLF radio fields. In: Nabighian, M.N. (Ed.), Electromagnetic Methods in Applied Geophysics, vol. 2, Application, part B. Society of Exploration Geophysicists, Tulsa, USA, pp. 521–640.

Mellqvist, C., Öhlander, B., Skiöld, T., Wikström, A., 1999. The Archaean–Proterozoic palaeoboundary in the Luleå area, northern Sweden: field and isotope geochemical evidence for a sharp terrane boundary. Precambrian Research 96, 225–243.

Nironen, M., 1997. The Svecofennian orogen: a tectonic model. Precambrian Research 86, 21–44.

Pares, J.M., van der Pluijm, B.A., 2002. Evaluating magnetic lineations (AMS) in deformed rocks. Tectonophysics 350, 283–298.

Smith, R.J., 2002. Geophysics of iron oxide copper–gold deposits. In: Porter, T.M. (Ed.), Hydrothermal Iron Oxide Copper–Gold and Related Deposits: A Global Perspective, vol. 2. Australian Mineral Foundation, Adelaide, pp. 357–367.

Tarling, D.H., Hrouda, F., 1993. The magnetic anisotropy of rocks. Chapman and Hall, London. 217 pp.

Wright, S.F., 1988. Early Proterozoic deformation history of the Kiruna District of northern Sweden. Unpublished Ph.D. thesis, University of Minnesota, 170 pp.